

---

# Neural Gromov-Wasserstein Optimal Transport

---

**Maksim Nekrashevich**

Skolkovo Institute of Science and Technology  
Moscow, Russia  
max.v.nekrashevich@gmail.com

**Alexander Korotin**

Skolkovo Institute of Science and Technology  
Artificial Intelligence Research Institute  
Moscow, Russia  
a.korotin@skoltech.ru

**Evgeny Burnaev**

Skolkovo Institute of Science and Technology  
Artificial Intelligence Research Institute  
Moscow, Russia  
e.burnaev@skoltech.ru

## Abstract

We present a scalable neural method to solve the Gromov-Wasserstein (GW) Optimal Transport (OT) problem with the inner product cost. In this problem, given two distributions supported on (possibly different) spaces, one has to find the most isometric map between them. Our proposed approach uses neural networks and stochastic mini-batch optimization which allows to overcome the limitations of existing GW methods such as their poor scalability with the number of samples and the lack of out-of-sample estimation. To demonstrate the effectiveness of our proposed method, we conduct experiments on the synthetic data and explore the practical applicability of our method to the popular task of the unsupervised alignment of word embeddings.

## 1 Introduction

Optimal Transport (OT) is a powerful framework that is widely used in machine learning [1]. A popular application of OT is the domain adaptation of various modalities including images [2–4], music transcription [5], color transfer [6], alignment of embedding spaces [7, 8]. Other applications include generative modeling [9, 10], unpaired image-to-image translation [11, 12], etc.

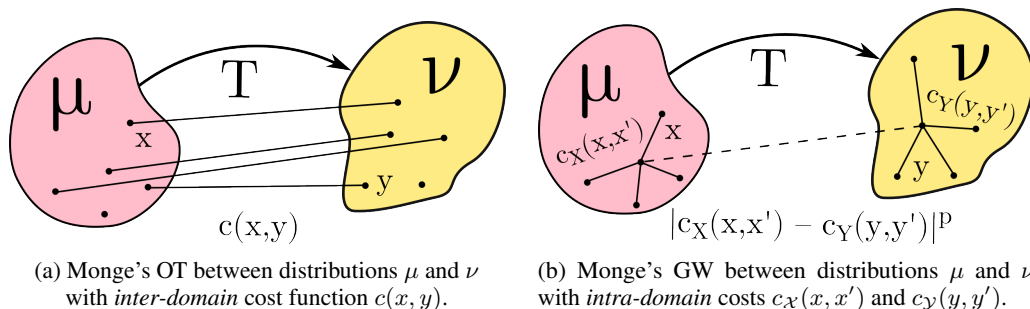


Figure 1: A schematic visualization of the OT problems and GW problems (Monge’s form).

In the OT problem (Figure 1 a), one needs to find a map between two data distributions that minimizes a certain “effort” expressed in the form of an *inter-domain* transport cost function. This cost function shows how hard to move a point of the source space to a given point of the target space. Thus, in

order for the resulting map to possess certain useful properties, one has to incorporate them into the cost function. Unfortunately, this is not always a straightforward task, especially when the data distributions are supported on different spaces.

A popular way to address the above-mentioned issue is to consider the Gromov-Wasserstein (GW) modification [13] of the OT problem (Figure 1b). Here one assumes that both the source and target spaces are equipped with a structure, e.g., with a metric, and one aims to find a transport map that maximally preserves this structure, i.e., the most isometric map. Unlike the conventional OT, GW is more easily applicable when the dimensions of the source and the target spaces are different as it does not require defining a cost function which operates on different spaces.

One of the most promising applications where GW shines is the task of unsupervised data alignment [7], in particular, aligning the datasets of word embeddings [14, 8]. Most methods that construct such an alignment require at least a small amount of paired data, see [15] for a survey. At the same time, several fully-unsupervised methods based on GW have been successfully applied to this task [14, 8].

Existing computational algorithms for GW are **discrete**, i.e., they work the source and target distributions that consist of a finite number of atoms. These methods have two **limitations**:

1. **Limited scalability.** Discrete GW methods can compute the map for distributions of the support size at most  $10^3 - 10^4$  samples. For higher support sizes the computation is costly. Thus, discrete methods are barely applicable to many real-world cases. For example, the datasets of word embeddings typically contain  $10^5 - 10^6$  words. Thus, the OT-based methods rely on certain heuristics, e.g., applying OT to a relatively small coreset rather than the whole dataset.
2. **No generalization.** Discrete GW methods perform the matching of train input with the target sample and do not provide the out-of-sample estimation for unseen data. However, this property is highly desirable in certain setups, e.g., online learning.

Recently, the usage of neural networks to solve OT problems has improved the scalability of OT methods and increased the range of their applications. Such neural OT methods can be roughly divided into two categories. The first category consists of methods that introduce the OT cost into the training loss of the neural network, mostly in the context of generative modeling [10, 16–19]. These are less related to the current study. The second category directly approximates the OT map between the distributions [20, 12, 21, 11, 22]. Yet all these methods consider conventional OT and do not straightforwardly extend to GW problem.

**Contributions.** We propose a novel algorithm for solving the GW problem based on neural networks (§4.1). Unlike the existing algorithms, our method scales well and allows doing the out-of-sample estimation. This development allows us to apply GW to aligning large-scale *unpaired* word embedding datasets which was unavailable for prior methods (§5.3). We also demonstrate the performance of our method on toy 2D/3D (§5.1) and Gaussian cases (§5.2).

**Notations.** We denote Polish spaces by capital calligraphic letters, e.g.,  $\mathcal{X}, \mathcal{Y}$ , and the corresponding sets of Borel probability distributions on them by  $P(\mathcal{X})$  and  $P(\mathcal{Y})$ . We denote the dot product of vectors in  $\mathbb{R}^D$  by  $\langle x, x' \rangle_D$ . For a measurable map  $T: \mathcal{X} \rightarrow \mathcal{Y}$ , we denote the corresponding *push-forward* operator by  $T_{\#}$ . We use  $f^c$  to denote the  $c$ -transform of  $f: \mathcal{Y} \rightarrow \mathbb{R}$  which is given by the formula  $f^c(y) = \min_{x \in \mathcal{X}} (c(x, y) - f(x))$ . For distributions  $\mu \in P(\mathcal{X})$  and  $\nu \in P(\mathcal{Y})$ , we denote the set of all couplings between them by  $\Pi(\mu, \nu)$ , i.e., distributions  $\pi$  on  $\mathcal{X} \times \mathcal{Y}$  with the corresponding marginals equal to  $\mu$  and  $\nu$ , respectively, i.e.,  $\int_{\mathcal{Y}} d\pi(x, y) = d\mu(x)$ ,  $\int_{\mathcal{X}} d\pi(x, y) = d\nu(y)$ .

## 2 Preliminaries

Here we describe the key concepts that we use throughout this paper. For a detailed overview of Optimal Transport, we refer to [23, 24], and of the Gromov-Wasserstein problem – to [25].

**Optimal Transport (OT) problem.** For distributions  $\mu \in P(\mathcal{X})$  and  $\nu \in P(\mathcal{Y})$  and a *cost* function  $c: \mathcal{X} \times \mathcal{Y} \rightarrow \mathbb{R}$ , consider the following optimization problem (Figure 1a):

$$\text{Cost}(\mu, \nu) \stackrel{\text{def}}{=} \min_{\substack{T: \mathcal{X} \rightarrow \mathcal{Y} \\ T_{\#}\mu = \nu}} \int_{\mathcal{X}} c(x, T(x)) d\mu(x). \quad (1)$$

Problem (1) is known as the *Monge's formulation of OT* and its solution  $T^*$  is called an OT map. For some  $\mu$  and  $\nu$ , there is no solution to this problem in the form of a deterministic map. Thus, it is common to consider the *Kantorovich's relaxation*

$$\text{Cost}(\mu, \nu) \stackrel{\text{def}}{=} \min_{\pi \in \Pi(\mu, \nu)} \int_{\mathcal{X} \times \mathcal{Y}} c(x, y) d\pi(x, y). \quad (2)$$

With mild assumptions on  $\mu, \nu$  and  $c$ , problem (2) admits a solution  $\pi^* \in \Pi(\mu, \nu)$  which is called an *OT plan*. In general, it may be non-unique. The dual problem to (2) is given by [23, Eq. 5.3]:

$$\text{Cost}(\mu, \nu) = \max_f \left[ \int_{\mathcal{X}} f^c(x) d\mu(x) + \int_{\mathcal{Y}} f(y) d\nu(y) \right], \quad (3)$$

where the supremum is taken over all integrable functions  $f: \mathcal{Y} \rightarrow \mathbb{R}$  and  $f^c$  is the  $c$ -transform of  $f$ .

**Neural dual [MM:R] solver for OT.** In practice, it is challenging to compute an OT map  $T^*$  in (1), especially when the distributions  $\mu$  and  $\nu$  are available only by empirical samples. Rather than solving the constrained primal formulation (1), recent methods [26, 12, 22] consider the dual formulation (3). They expand  $f^c$  using its definition to get the following equivalent optimization problem:

$$\text{Cost}(\mu, \nu) = \max_f \min_{T: \mathcal{X} \rightarrow \mathcal{Y}} \left[ \int_{\mathcal{X}} c(x, T(x)) - f(T(x)) d\mu(x) \right] + \int_{\mathcal{Y}} f(y) d\nu(y), \quad (4)$$

see [26, §2] or [12, §4.1] for a more detailed explanation. There also exists a modification that allows to implicitly recover the OT plan  $\pi^*$  from the solution of (4), see [11].

**Gromov-Wasserstein (GW) problem.** Suppose that for  $\mathcal{X}$  and  $\mathcal{Y}$  instead of an “inter-domain” cost function  $c(x, y)$ , i.e., a function that assigns a value for pairs  $(x, y) \in \mathcal{X} \times \mathcal{Y}$ , there are two “intra-domain” cost functions  $c_{\mathcal{X}}: \mathcal{X} \times \mathcal{X} \rightarrow \mathbb{R}$  and  $c_{\mathcal{Y}}: \mathcal{Y} \times \mathcal{Y} \rightarrow \mathbb{R}$ . Fix a parameter  $p \geq 1$  and consider the following Monge's GW problem (Figure 1b):

$$\text{GW}_p^p(\mu, \nu) \stackrel{\text{def}}{=} \min_{\substack{T: \mathcal{X} \rightarrow \mathcal{Y} \\ T_{\#}\mu = \nu}} \iint_{\mathcal{X} \times \mathcal{X}} \left| c_{\mathcal{X}}(x, x') - c_{\mathcal{Y}}(T(x), T(x')) \right|^p d\mu(x) d\mu(x'), \quad (5)$$

While in (1) we search for a map that sends  $\mu$  to  $\nu$  minimizing the transport cost, (5) aims to find the most isometric map w.r.t. the costs  $c_{\mathcal{X}}$  and  $c_{\mathcal{Y}}$ , i.e., the map that maximally preserves the pairwise intra-domain costs. Similar to (1), problem (5) admits the following Kantorovich's GW relaxation:

$$\text{GW}_p^p(\mu, \nu) \stackrel{\text{def}}{=} \min_{\pi \in \Pi(\mu, \nu)} \iint_{(\mathcal{X} \times \mathcal{X})^2} \left| c_{\mathcal{X}}(x, x') - c_{\mathcal{Y}}(y, y') \right|^p d\pi(x, y) d\pi(x', y'). \quad (6)$$

Formulations (5) and (6) more suitable than (1) and (2) for distributions that are supported on different spaces as it relies only on the intra-domain cost functions  $c_{\mathcal{X}}$  and  $c_{\mathcal{Y}}$ . In contrast, to apply OT (2) in this setting, one has to manually define an inter-domain cost function  $c(x, y)$  *between* the two spaces, which is not a trivial task. However, the solution of the GW problem is determined up to the isometries of the source and the target space, i.e., maps on each space that preserve both the respective distributions and the cost functions.

**The inner product case.** Henceforth, we consider the special case of (6) called the *inner product GW*. It corresponds to the setting when  $\mathcal{X} = \mathbb{R}^m$ ,  $\mathcal{Y} = \mathbb{R}^n$ ,  $c_{\mathcal{X}} = \langle \cdot, \cdot \rangle_m$ ,  $c_{\mathcal{Y}} = \langle \cdot, \cdot \rangle_n$  and  $p = 2$ :

$$\text{innerGW}^2(\mu, \nu) \stackrel{\text{def}}{=} \min_{\substack{T: \mathcal{X} \rightarrow \mathcal{Y} \\ T_{\#}\mu = \nu}} \iint_{\mathcal{X} \times \mathcal{X}} \left| \langle x, x' \rangle_m - \langle T(x), T(x') \rangle_n \right|^2 d\mu(x) d\mu(x'). \quad (7)$$

This case is particularly useful for aligning the spaces of embeddings. For example, word embeddings are typically learned by optimizing the cosine similarity. Moreover, it is a common practice to normalize the embeddings, so that the embedding vectors have unit length [27, §3.3], [28, §2.4]. In this case, the cosine similarity becomes equivalent to the inner product. Thus, the solution to (7) by design maximally preserves the internal structure of the embedding space w.r.t. the cosine similarity.

### 3 Related work

#### 3.1 Computation of OT and GW Transport Maps

Most existing computational OT methods are designed for *discrete* distributions, see [29] for a survey. These methods by design do matching between the empirical datasets and do not provide out-of-sample estimation. In particular, Gromov-Wasserstein problem is extensively covered in [25]. This issues is addressed by *continuous* (a.k.a. parametric or neural) methods [20, 30, 12], see [26] for a survey and a benchmark. According to the authors, the best performing method is the [MM:R] which is based on the saddle point reformulation (4) of the dual problem. Originally, this method was designed for OT (1) with the quadratic cost  $c(x, y) = \|x - y\|_2^2$  [26] but later extended to more general costs [12, 31, 11, 22, 32]. Yet it considers the conventional OT problems but is not straightforward applicable to GW. In this paper, we show how [MM:R] can be applied to GW problem.

#### 3.2 Embedding Alignment

There are numerous approaches to solve embedding alignment, most of which require training on parallel data. These methods either rely on solving least-squares to find the mapping [33], or solve the orthogonal procrustes problem [34]. Optimal Transport falls into the category of unsupervised methods. The works [35], [8], and [14] leverage discrete OT and discrete GW to solve the task of word embedding alignment.

### 4 Neural Algorithm for Gromov-Wasserstein

In this section, we propose a novel scalable method to solve the innerGW problem (7). We base our method on the theoretical insights about GW of [25] and the neural OT solver (4) by [26].

According to [25, Theorem 4.2.1], when  $\int \|x\|_2^4 d\mu(x) < +\infty$ ,  $\int \|y\|_2^4 d\nu(y) < +\infty$ , the problem (7) is equivalent to the following problem:

$$\text{innerGW}^2(\mu, \nu) = \text{Const}(\mu, \nu) - \max_{\substack{\pi \in \Pi(\mu, \nu) \\ P \in F_{m,n}}} \int \langle Px, y \rangle_n d\pi(x, y), \quad (8)$$

where  $F_{m,n} \stackrel{\text{def}}{=} \{P \in \mathbb{R}^{n \times m} \mid \|P\|_{\mathcal{F}} = \min(\sqrt{m}, \sqrt{n})\}$  is the space of matrices of the fixed Frobenius norm. Inspired by [26], we propose a neural algorithm to solve (6).

**Lemma 4.1** (InnerGW as a minimax optimization). *It holds that (5) is equivalent to*

$$\text{innerGW}^2(\mu, \nu) = \text{Const}(\mu, \nu) + \min_{P \in F_{m,n}} \max_f \min_{\substack{T: \mathbb{R}^m \rightarrow \mathbb{R}^n \\ T\# \mu = \nu}} \mathcal{L}(P, f, T), \quad (9)$$

where

$$\mathcal{L}(P, f, T) \stackrel{\text{def}}{=} \int_{\mathbb{R}^n} f(y) d\nu(y) - \int_{\mathbb{R}^m} [\langle Px, T(x) \rangle_n + f(T(x))] d\mu(x). \quad (10)$$

*Proof.* We start with (8). For each  $P$ , we rewrite the inner optimization over  $P$  following (4):

$$\begin{aligned} \max_{\substack{\pi \in \Pi(\mu, \nu) \\ P \in F_{m,n} \mathbb{R}^m \times \mathbb{R}^n}} \int \langle Px, y \rangle_n d\pi(x, y) &= \max_{P \in F_{m,n}} \max_{\pi \in \Pi(\mu, \nu)} \int_{\mathbb{R}^m \times \mathbb{R}^n} \langle Px, y \rangle_n d\pi(x, y) = \\ &= \min_{P \in F_{m,n}} \left[ \min_{\pi \in \Pi(\mu, \nu)} \int_{\mathbb{R}^m \times \mathbb{R}^n} -\langle Px, y \rangle_n d\pi(x, y) \right] = \end{aligned} \quad (11)$$

$$\begin{aligned} &= \min_{P \in F_{m,n}} \left[ \max_f \int_{\mathbb{R}^n} f(y) d\nu(y) + \min_{T: \mathbb{R}^m \rightarrow \mathbb{R}^n} \int_{\mathbb{R}^m} -\langle Px, T(x) \rangle_n - f(T(x)) d\mu(x) \right] = \\ &= \min_{P \in F_{m,n}} \max_f \min_{T: \mathbb{R}^m \rightarrow \mathbb{R}^n} \mathcal{L}(P, f, T). \end{aligned} \quad (12)$$

The equality in transition from line (11) follows from (2) and (3) applied to the cost function  $c(x, y) = -\langle Px, y \rangle_n$ .  $\square$

**Theorem 4.2** (Optimal maps solve the minimax problem). *Assume that there exists at least one GW map  $T^*$ . For any matrix  $P^*$  and a potential  $f^*$  that solve (9), i.e.,  $P^* \in \operatorname{argmin}_{P \in F_{m,n}} \max_f \min_{T: \mathbb{R}^m \rightarrow \mathbb{R}^n} \mathcal{L}(P, f, T)$  and  $f^* \in \operatorname{argmax}_f \min_{T: \mathbb{R}^m \rightarrow \mathbb{R}^n} \mathcal{L}(P^*, f, T)$ , and for any GW map  $T^*$ , we have:*

$$T^* \in \operatorname{argmin}_{T: \mathbb{R}^m \rightarrow \mathbb{R}^n} \mathcal{L}(P^*, f^*, T). \quad (13)$$

*Proof.* To show this, we expand  $\mathcal{L}(P^*, f^*, T^*)$  by definition and use the fact that  $T^*$  is the OT map.

$$\mathcal{L}(P^*, f^*, T^*) = \int_{\mathbb{R}^n} f^*(y) d\nu(y) - \int_{\mathbb{R}^m} \langle P^* x, T^*(x) \rangle + f^*(T^*(x)) d\mu(x). \quad (14)$$

Since  $T^*$  is an OT map, we have  $T^*_{\#} \mu = \nu$ , and by the change of variables formula we get:

$$\int_{\mathbb{R}^m} f^*(T^*(x)) d\mu(x) = \int_{\mathbb{R}^n} f^*(y) d\nu(y). \quad (15)$$

Plugging this into (14), we get:

$$\mathcal{L}(P^*, f^*, T^*) = - \int_{\mathbb{R}^m} \langle P^* x, T^*(x) \rangle d\mu(x). \quad (16)$$

Here, we once again use the fact that  $T^*$  is the optimal transport map. Now, since  $P^*$  and  $f^*$  solve (9), we get the following:

$$\operatorname{innerGW}^2(\mu, \nu) = \operatorname{Const}(\mu, \nu) + \min_{\substack{T: \mathbb{R}^m \rightarrow \mathbb{R}^n \\ T_{\#} \mu = \nu}} \mathcal{L}(P^*, f^*, T) \quad (17)$$

Finally, from the fact that  $\pi^* = [id_{\mathbb{R}^m}, T^*]_{\#} \mu$  is optimal and (11), we have:

$$\begin{aligned} -\mathcal{L}(P^*, f^*, T^*) &= \int_{\mathbb{R}^m \times \mathbb{R}^n} \langle P^* x, y \rangle d\pi^*(x, y) = \max_{\pi \in \Pi(\mu, \nu)} \int_{\mathbb{R}^m \times \mathbb{R}^n} \langle P^* x, y \rangle_n d\pi(x, y) = \\ &= \min_{\substack{T: \mathbb{R}^m \rightarrow \mathbb{R}^n \\ T_{\#} \mu = \nu}} \mathcal{L}(P^*, f^*, T), \end{aligned} \quad (18)$$

which completes the proof.  $\square$

## 4.1 Optimization procedure

We parameterize  $f$  and  $T$  with neural networks and  $P$  with a matrix of the fixed Frobenius norm. This enables us to solve (9) using an alternating stochastic gradient optimization. It involves performing the gradient optimization steps for  $f$ ,  $T$  and  $P$  sequentially. Each step consists of approximating the integrals in (9) using Monte Carlo sampling and then updating the parameters according to the gradient. At each iteration, we first do  $k_P$  steps for  $P$ , and then, for each of  $k_f$  steps of  $f$  we perform  $k_T$  steps for  $T$ . The optimization procedure is summarized in Algorithm 1.

---

### Algorithm 1: Neural Gromov-Wasserstein (NGW)

---

**Input:** distributions  $\mu$  and  $\nu$  on  $\mathbb{R}^m$  and  $\mathbb{R}^n$ , respectively, accessible by samples.

**Output:** innerGW optimal transport map  $T^*$ .

**Parameters :** potential network  $f: \mathbb{R}^n \rightarrow \mathbb{R}$ , transport network  $T: \mathbb{R}^m \rightarrow \mathbb{R}^n$ , matrix  $P \in F_{m,n}$ , associated with the cost.  
number of steps  $k_f, k_T, k_P$ , for  $f, T$  and  $P$ , respectively.

```

repeat
  repeat  $k_P$  times
    Sample batches  $X \sim \mu$  and  $Y \sim \nu$ ;
    Apply the transport network  $Z = T(X)$ ;
    Compute the cost loss  $\mathcal{L}_P \leftarrow -\frac{1}{|X|} \sum_j \langle P x_j, z_j \rangle_n$ ;
    Update  $P$  using  $\nabla_P \mathcal{L}_P$ ;
  end
  repeat  $k_f$  times
    repeat  $k_T$  times
      Sample batches  $X \sim \mu, Y \sim \nu$ ;
      Apply the transport network  $Z = T(X)$ ;
      Compute the transport loss  $\mathcal{L}_T \leftarrow -\frac{1}{|X|} \sum_j \langle P x_j, z_j \rangle_n - \frac{1}{|Z|} \sum_{z \in Z} f(z)$ ;
      Update  $T$  using  $\nabla_T \mathcal{L}_T$ ;
    end
    Sample batches  $X \sim \mu, Y \sim \nu$ ;
    Apply the transport network  $Z = T(X)$ ;
    Compute the potential loss  $\mathcal{L}_f \leftarrow \frac{1}{|Z|} \sum_{z \in Z} f(z) - \frac{1}{|Y|} \sum_{y \in Y} f(y)$ ;
    Update  $f$  using  $\nabla_f \mathcal{L}_f$ ;
  end
end
until converged;

```

---

## 5 Experiments

In §5.1, we provide the results of experiments on synthetic low-dimensional data. This allows us to qualitatively evaluate the method. In §5.2, we conduct experiments on multivariate normal distributions. In this case, the ground truth is known, i.e., we can qualitatively assess the performance of our method. In §5.3 we test our method on the downstream task of word embedding alignment.

The experiments are conducted using PyTorch framework. The code will be made publicly available.

### 5.1 Toy Examples

To begin with, we test our algorithm on a set of toy examples. For each experiment we provide two random initializations to show that the transport map is reconstructed up to rotations of both spaces.

In our first experiment,  $\mu$  and  $\nu$  are two mixtures in  $\mathbb{R}^2$  of Gaussian distributions with 10 and 5 components, respectively, which are uniformly spread around a unit circle (Figures 2a and 2b). In Figures 2d to 2f we show the learned transport between them. We see that two neighboring components expectedly get mapped either to the same component or to the neighboring components of the target distribution.

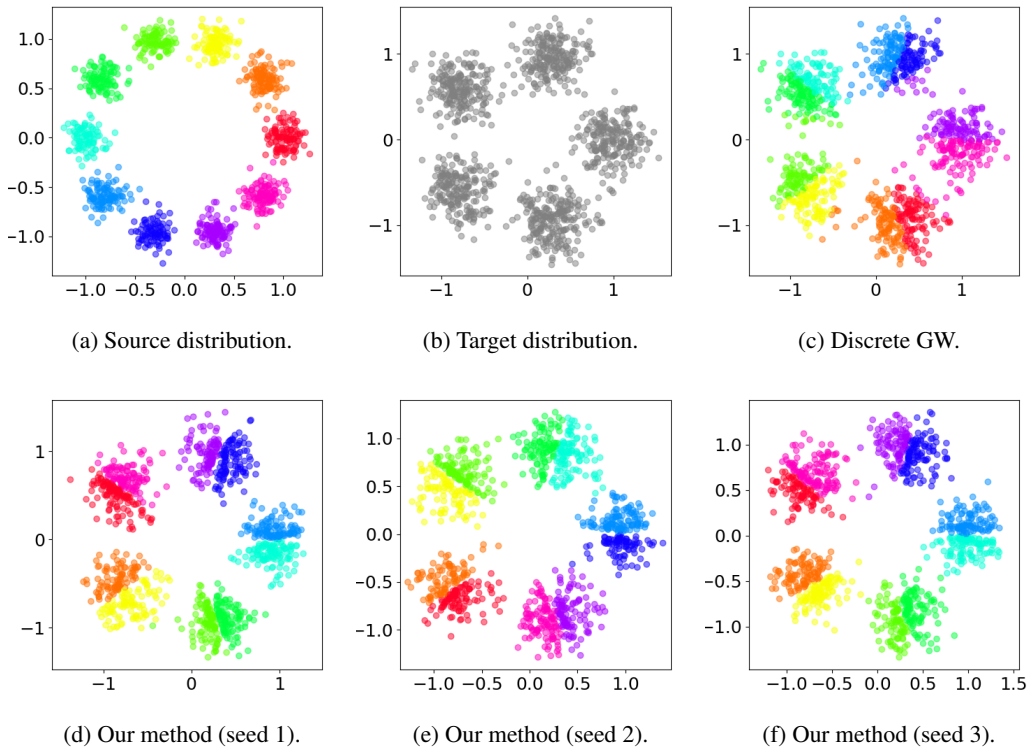


Figure 2: GW transport between Gaussian mixtures in  $\mathbb{R}^2$ .

Secondly, to test our method in unequal dimensions, we consider the transport between spaces of different dimensions. We take Gaussian mixtures of eight components in  $\mathbb{R}^3$  and  $\mathbb{R}^2$ , respectively. In  $\mathbb{R}^3$ , the source components are located in the vertices of a cube (Figure 3a) while in  $\mathbb{R}^2$ , the components of the target mixture are spread uniformly on a unit circle (Figure 3b). In this case, both the source and target distributions have many symmetries, so the resulting map again depends on the initialization. As in the first case, we see that a component of the source distribution is mostly mapped to a component of the target distribution (Figures 3d to 3f).

For completeness, for all the pairs  $\mu, \nu$ , we also provide the results of an alignment between two empirical samples from the distributions using the discrete Gromov-Wasserstein from Python Optimal Transport (POT) package<sup>1</sup> (`ot.gromov.gromov_wasserstein`), see Figures 2c and 3c.

## 5.2 Multivariate Normal distributions in $\mathbb{R}^n$

We proceed with the case when  $\mu$  and  $\nu$  are Gaussian distributions. It is a rare case when the GW problem can be solved analytically. Therefore, we can compare the results of our algorithm with the ground truth GW map. In [36], the authors obtain a lower bound on Gromov-Wasserstein discrepancy between Gaussian distributions and the closed form solution for the GW OT map. Although they consider the case of the quadratic costs  $c_{\mathcal{X}}(x, x') = \|x - x'\|_m^2$  and  $c_{\mathcal{Y}}(y, y') = \|y - y'\|_n^2$ , similar results can be obtained for the case of innerGW (7). For completeness of the exposition, we show how their result can be adapted to the inner-product GW.

**Lemma 5.1** (InnerGW between Gaussian distributions). *Suppose that  $m \geq n$ ,  $\mu = \mathcal{N}(0, \Sigma_\mu) \in P(\mathbb{R}^m)$ ,  $\nu = \mathcal{N}(0, \Sigma_\nu) \in P(\mathbb{R}^n)$  and suppose that  $\Sigma_\mu = P_\mu^T D_\mu P_\mu$ ,  $\Sigma_\nu = P_\nu^T D_\nu P_\nu$  - diagonaliza-*

<sup>1</sup><https://pythonot.github.io>

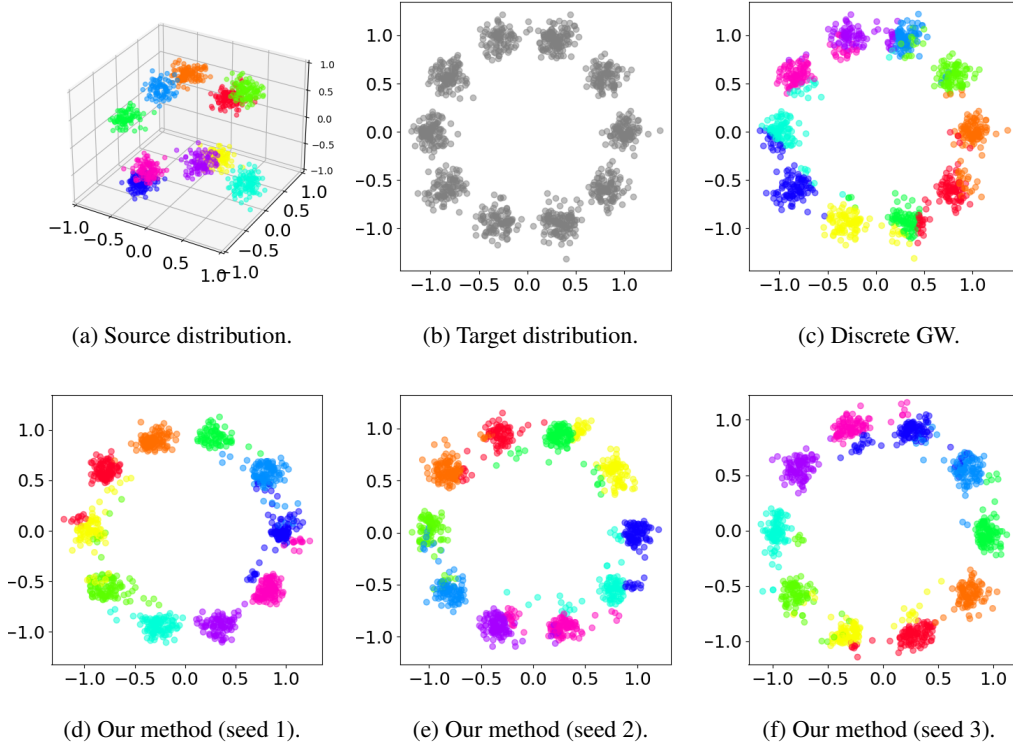


Figure 3: GW transport between Gaussian mixtures in  $\mathbb{R}^3$  and  $\mathbb{R}^2$ , respectively.

tions of  $\Sigma_\mu$  and  $\Sigma_\nu$ , respectively, i.e.,  $P_\mu$  and  $P_\nu$  are rotation matrices and  $D_\mu$  and  $D_\nu$  are diagonal. Then innerGW<sup>2</sup> is given by the following formula:

$$\text{innerLGW}^2(\mu, \nu) = \text{tr}(D_\mu^2) + \text{tr}(D_\nu^2) - 2 \text{tr}((D_\mu)_{\leq n} D_\nu), \quad (19)$$

where  $(D_\mu)_{\leq n}$  is a diagonal matrix that consists of  $n$  largest eigenvalues of  $D_\mu$ . And the optimal maps  $T^*$  in this case are given by  $T^*(x) = P_\nu A P_\mu x$  where  $A = \left( \tilde{I}_n D_\nu^{\frac{1}{2}} ((D_\mu)_{\leq n})^{-\frac{1}{2}}, 0 \right) \in \mathbb{R}^{n \times m}$  and  $\tilde{I}_n$  is an arbitrary diagonal matrix with entries  $\pm 1$ .

Thanks to our lemma, we can quantitatively compare our method with the ground truth. We define  $\mu$  and  $\nu$  to be Gaussian distributions with zero mean and the covariance matrix  $\Sigma = P^T D P$ , where  $P$  is a random rotation matrix and the entries of  $D$  are chosen uniformly from the interval  $[\frac{1}{2}, 2]$ .

**Metrics.** First, to determine, whether the resulting map minimizes (6), we compute the empirical estimate the target functional innerGW and report it together with the ground truth value. Here we do not use a specific metric. Second, to compare how well the image of the source distribution under our map  $T$  matches the target distribution, we report the Bures-Wasserstein unexplained variance percentage ( $\text{BW}_2^2\text{-UVP}$ ) [37], which is defined as follows:

$$\text{BW}_2^2\text{-UVP}(T) \stackrel{\text{def}}{=} \frac{\text{BW}_2^2(T\#\mu, \nu)}{\frac{1}{2} \text{Var } \nu} \cdot 100\%, \quad (20)$$

where  $\text{BW}_2^2(\mu, \nu) = \mathbb{W}_2^2(\mathcal{N}(m_\mu, \Sigma_\mu), \mathcal{N}(m_\nu, \Sigma_\nu))$  admits a closed form solution [38].

**Baselines.** We also show the results of the discrete Gromov-Wasserstein method from POT by training a transport between two empirical samples of 2000 points from the Gaussians. This method *cannot* perform out-of-sample estimation, so we come up with the following baseline. We fit a linear regression over the obtained transport plan between empirical samples and use it as an approximation



DIM		INNERGW				BW <sub>2</sub> <sup>2</sup> -UVP	
SRC	TGT	GT	DISCRETE	DISCRETE+LR	NGW	DISCRETE+LR	NGW
1024	256	1024.04	2685.53	1635.45	<b>1553.3</b>	<b>0.28</b>	1.1
	64	1569.59	2586.22	1700.46	<b>1588.04</b>	0.07	0.07
	16	1722.41	2528.08	1747.05	<b>1721.4</b>	0.04	<b>0.02</b>
	4	1761.95	2547.26	1766.21	<b>1757.98</b>	0.20	<b>0.01</b>
256	256	0.95	866.52	<b>346.60</b>	741.85	<b>1.01</b>	1.32
	64	266.18	538.10	386.12	<b>313.25</b>	<b>0.50</b>	0.97
	16	398.03	466.66	415.71	<b>398.79</b>	0.19	<b>0.02</b>
	4	433.04	471.44	<b>430.39</b>	432.18	0.07	<b>0.01</b>
64	64	1.07	186.66	<b>67.38</b>	104.53	<b>0.83</b>	1.44
	16	67.77	102.09	84.60	<b>72.36</b>	0.21	<b>0.03</b>
	4	99.59	102.32	101.41	<b>99.42</b>	0.04	<b>0.02</b>
16	16	1.56	26.29	<b>8.73</b>	9.31	<b>0.28</b>	1.0
	4	19.4	20.61	<b>19.54</b>	19.92	<b>0.01</b>	0.02
4	4	1.76	1.42	0.59	<b>0.9</b>	<b>0.01</b>	0.02

Table 1: The comparison of NGW (our method) with the discrete GW and Linear Regression fitted over discrete GW plan (baseline) in the Gaussian case.

CORPUS	DIM		ACCURACY		
	SRC	TGT	TOP-1	TOP-5	TOP-10
WIKI	200	100	0.98	0.99	0.99
	100	50	0.95	0.99	0.98
TWITTER	200	100	0.86	0.94	0.92
	100	50	0.71	0.86	0.83
	50	25	0.37	0.63	0.56

Table 2: Accuracy scores of the alignment of GloVe embeddings across different dimensions.

of the of the GWOT map. We estimate the GW discrepancy between the distributions by sampling additional 2048 points. The resulting metrics are shown in Table 1. We see that our method achieves better results in most of the setups, especially, in higher dimensions.

### 5.3 Alignment of Word Embeddings

Finally, we consider the downstream task of word embedding alignment. We measure the quality of the alignment using top- $k$  accuracy ( $k = 1, 5, 10$ ).

**GloVe.** We consider the sets of embeddings of different dimensions of the GLoVe [39] language model trained on Twitter and Wiki corpora. Our hypothesis is that since the texts are the same, it is possible to learn a very good alignment. The results are given in Table 2.

**MUSE.** To test the out-of-distribution prediction capabilities of NGW, we consider a real-world dataset MUSE [40]. It is comprised of fastText word embeddings [41] and bilingual dictionaries for English (EN), French (FR), German (DE), Italian (IT), Portuguese (PT), and Spanish (ES) languages. This setup is more complicated as the ground truth alignment is not one-to-one.

For each pair of languages, we split *source* set of embeddings into the train (80%) and test parts (20%). We apply NGW to align the train source dataset with the *entire* target dataset. We then measure the quality of alignment using top- $k$  accuracy on both splits. The results are given in Table 3. We observe almost identical results for the train and out-of-distribution metrics.

**Remark.** We failed to reproduce the results of [14] in the same setup. We will provide a more extensive comparison of NGW with the existing alignment methods in the next version of our note.

LANG		ACCURACY (TRAIN)			ACCURACY (OOD)		
SRC	TGT	TOP-1	TOP-5	TOP-10	TOP-1	TOP-5	TOP-10
DE	EN	0.262	0.497	0.585	0.256	0.498	0.587
	ES	0.235	0.453	0.540	0.235	0.449	0.537
	FR	0.302	0.514	0.601	0.297	0.509	0.592
	IT	0.246	0.446	0.533	0.247	0.443	0.530
	PT	0.214	0.399	0.486	0.207	0.392	0.478
EN	DE	0.306	0.531	0.617	0.300	0.534	0.616
	ES	0.283	0.508	0.595	0.273	0.504	0.590
	FR	0.226	0.431	0.517	0.227	0.427	0.512
	IT	0.242	0.453	0.540	0.238	0.443	0.532
	PT	0.186	0.367	0.449	0.179	0.358	0.440
ES	DE	0.265	0.474	0.561	0.261	0.468	0.554
	EN	0.275	0.502	0.587	0.271	0.497	0.579
	FR	0.319	0.530	0.615	0.315	0.523	0.605
	IT	0.303	0.510	0.593	0.295	0.503	0.586
	PT	0.360	0.564	0.639	0.353	0.558	0.631
FR	DE	0.340	0.553	0.634	0.334	0.547	0.631
	EN	0.299	0.529	0.614	0.298	0.527	0.611
	ES	0.318	0.519	0.602	0.321	0.526	0.609
	IT	0.274	0.476	0.558	0.265	0.473	0.555
	PT	0.225	0.407	0.485	0.218	0.400	0.479
IT	DE	0.305	0.511	0.594	0.292	0.503	0.589
	EN	0.206	0.402	0.487	0.199	0.394	0.478
	ES	0.335	0.546	0.625	0.333	0.541	0.621
	FR	0.325	0.531	0.615	0.319	0.520	0.604
	PT	0.273	0.465	0.545	0.268	0.459	0.540
PT	DE	0.243	0.425	0.506	0.237	0.425	0.506
	EN	0.191	0.383	0.464	0.187	0.378	0.462
	ES	0.398	0.597	0.670	0.393	0.599	0.670
	FR	0.209	0.391	0.474	0.203	0.382	0.467
	IT	0.255	0.447	0.529	0.252	0.437	0.518

Table 3: The train and out-of-distribution accuracy of the alignment between English (EN), French (FR), German (DE), Italian (IT), Portuguese (PT), and Spanish (ES) languages.

## 6 Limitations

We focus on the case of GW with the inner product cost function and  $p = 2$ . Additionally, we do not guarantee that for all the optimal saddle points  $(P^*, f^*, T^*)$  of (11) it holds that  $T^*$  is an OT map. Extending our algorithm to more general cases of GW and removing the ambiguity in saddle points is a promising future research avenue.

## References

- [1] Luis Caicedo Torres, Luiz Manella Pereira, and M Hadi Amini. A survey on optimal transport for machine learning: Theory and applications. *arXiv preprint arXiv:2106.01963*, 2021.
- [2] Nicolas Courty, Rémi Flamary, Devis Tuia, and Alain Rakotomamonjy. Optimal transport for domain adaptation. *IEEE transactions on pattern analysis and machine intelligence*, 39(9): 1853–1865, 2016.
- [3] Yun Luo, Si-Yang Zhang, Wei-Long Zheng, and Bao-Liang Lu. WGAN domain adaptation for eeg-based emotion recognition. In *International Conference on Neural Information Processing*, pages 275–286. Springer, 2018.

- [4] Ievgen Redko, Nicolas Courty, Rémi Flamary, and Devis Tuia. Optimal transport for multi-source domain adaptation under target shift. *arXiv preprint arXiv:1803.04899*, 2018.
- [5] Rémi Flamary, Cédric Févotte, Nicolas Courty, and Valentin Emiya. Optimal spectral transportation with application to music transcription. *Advances in Neural Information Processing Systems*, 29, 2016.
- [6] Oriel Frigo, Neus Sabater, Vincent Demoulin, and Pierre Hellier. Optimal transportation for example-guided color transfer. In *Computer Vision—ACCV 2014: 12th Asian Conference on Computer Vision, Singapore, Singapore, November 1-5, 2014, Revised Selected Papers, Part III 12*, pages 655–670. Springer, 2015.
- [7] Liqun Chen, Zhe Gan, Yu Cheng, Linjie Li, Lawrence Carin, and Jingjing Liu. Graph optimal transport for cross-domain alignment. In *International Conference on Machine Learning*, pages 1542–1553. PMLR, 2020.
- [8] Prince O Aboagye, Yan Zheng, Michael Yeh, Junpeng Wang, Zhongfang Zhuang, Huiyuan Chen, Liang Wang, Wei Zhang, and Jeff Phillips. Quantized wasserstein procrustes alignment of word embedding spaces. *arXiv preprint arXiv:2212.02468*, 2022.
- [9] Tim Salimans, Han Zhang, Alec Radford, and Dimitris Metaxas. Improving gans using optimal transport. *arXiv preprint arXiv:1803.05573*, 2018.
- [10] Martin Arjovsky, Soumith Chintala, and Léon Bottou. Wasserstein GAN. *arXiv preprint arXiv:1701.07875*, 2017.
- [11] Alexander Korotin, Daniil Selikhanovych, and Evgeny Burnaev. Neural optimal transport. *arXiv preprint arXiv:2201.12220*, 2022.
- [12] Litu Rout, Alexander Korotin, and Evgeny Burnaev. Generative modeling with optimal transport maps. In *International Conference on Learning Representations*, 2022. URL <https://openreview.net/forum?id=5JdLZg346Lw>.
- [13] M Botsch and R Pajarola. On the use of gromov-hausdorff distances for shape comparison.
- [14] David Alvarez-Melis and Tommi S Jaakkola. Gromov-wasserstein alignment of word embedding spaces. *arXiv preprint arXiv:1809.00013*, 2018.
- [15] Sebastian Ruder, Ivan Vulić, and Anders Søgaard. A survey of cross-lingual word embedding models. *Journal of Artificial Intelligence Research*, 65:569–631, 2019.
- [16] Ishaan Gulrajani, Faruk Ahmed, Martin Arjovsky, Vincent Dumoulin, and Aaron C Courville. Improved training of Wasserstein GANs. In *Advances in Neural Information Processing Systems*, pages 5767–5777, 2017.
- [17] Huidong Liu, Xianfeng Gu, and Dimitris Samaras. Wasserstein GAN with quadratic transport cost. In *Proceedings of the IEEE International Conference on Computer Vision*, pages 4832–4841, 2019.
- [18] Maziar Sanjabi, Jimmy Ba, Meisam Razaviyayn, and Jason D Lee. On the convergence and robustness of training GANs with regularized optimal transport. *arXiv preprint arXiv:1802.08249*, 2018.
- [19] Henning Petzka, Asja Fischer, and Denis Lukovnicov. On the regularization of wasserstein gans. *arXiv preprint arXiv:1709.08894*, 2017.
- [20] Vivien Seguy, Bharath Bhushan Damodaran, Rémi Flamary, Nicolas Courty, Antoine Rolet, and Mathieu Blondel. Large-scale optimal transport and mapping estimation. *arXiv preprint arXiv:1711.02283*, 2017.
- [21] Grady Daniels, Tyler Maunu, and Paul Hand. Score-based generative neural networks for large-scale optimal transport. *Advances in Neural Information Processing Systems*, 34, 2021.
- [22] Jiaojiao Fan, Shu Liu, Shaojun Ma, Yongxin Chen, and Haomin Zhou. Scalable computation of monge maps with general costs. *arXiv preprint arXiv:2106.03812*, 2021.

- [23] Cédric Villani. *Optimal transport: old and new*, volume 338. Springer Science & Business Media, 2008.
- [24] Filippo Santambrogio. Optimal transport for applied mathematicians. *Birkäuser, NY*, 55(58-63): 94, 2015.
- [25] Titouan Vayer. A contribution to optimal transport on incomparable spaces. *arXiv preprint arXiv:2011.04447*, 2020.
- [26] Alexander Korotin, Lingxiao Li, Aude Genevay, Justin M Solomon, Alexander Filippov, and Evgeny Burnaev. Do neural optimal transport solvers work? a continuous wasserstein-2 benchmark. *Advances in Neural Information Processing Systems*, 34, 2021.
- [27] Omer Levy, Yoav Goldberg, and Ido Dagan. Improving distributional similarity with lessons learned from word embeddings. *Transactions of the association for computational linguistics*, 3:211–225, 2015.
- [28] Alec Radford, Jong Wook Kim, Chris Hallacy, Aditya Ramesh, Gabriel Goh, Sandhini Agarwal, Girish Sastry, Amanda Askell, Pamela Mishkin, Jack Clark, et al. Learning transferable visual models from natural language supervision. In *International Conference on Machine Learning*, pages 8748–8763. PMLR, 2021.
- [29] Gabriel Peyré, Marco Cuturi, et al. Computational optimal transport. *Foundations and Trends® in Machine Learning*, 11(5-6):355–607, 2019.
- [30] Ashok Vardhan Makkuva, Amirhossein Taghvaei, Sewoong Oh, and Jason D Lee. Optimal transport mapping via input convex neural networks. *arXiv preprint arXiv:1908.10962*, 2019.
- [31] Milena Gazdieva, Litu Rout, Alexander Korotin, Andrey Kravchenko, Alexander Filippov, and Evgeny Burnaev. An optimal transport perspective on unpaired image super-resolution. *arXiv preprint arXiv:2202.01116*, 2022.
- [32] Arip Asadulaev, Alexander Korotin, Vage Egiazarian, and Evgeny Burnaev. Neural optimal transport with general cost functionals. *arXiv preprint arXiv:2205.15403*, 2022.
- [33] David M Gaddy, Yuan Zhang, Regina Barzilay, and Tommi S Jaakkola. Ten pairs to tag-multilingual pos tagging via coarse mapping between embeddings. *Association for Computational Linguistics*, 2016.
- [34] Alexis Conneau, Guillaume Lample, Marc’Aurelio Ranzato, Ludovic Denoyer, and Hervé Jégou. Word translation without parallel data. *arXiv preprint arXiv:1710.04087*, 2017.
- [35] Meng Zhang, Yang Liu, Huanbo Luan, and Maosong Sun. Earth mover’s distance minimization for unsupervised bilingual lexicon induction. In *Proceedings of the 2017 Conference on Empirical Methods in Natural Language Processing*, pages 1934–1945, 2017.
- [36] Antoine Salmona, Julie Delon, and Agnès Desolneux. Gromov-wasserstein distances between gaussian distributions. *arXiv preprint arXiv:2104.07970*, 2021.
- [37] Alexander Korotin, Vage Egiazarian, Arip Asadulaev, Alexander Safin, and Evgeny Burnaev. Wasserstein-2 generative networks. In *International Conference on Learning Representations*, 2021. URL [https://openreview.net/forum?id=bEoxzW\\_EXsa](https://openreview.net/forum?id=bEoxzW_EXsa).
- [38] Aicke Hinrichs and Lev Markhasin. On lower bounds for the l2-discrepancy. *Journal of Complexity*, 27(2):127–132, 2011.
- [39] Richard Socher, Jeffrey Pennington, and Christopher D Manning. Glove: Global vectors for word representation. In *Conference on Empirical Methods in Natural Language Processing*. Citeseer, 2014.
- [40] Guillaume Lample, Alexis Conneau, Ludovic Denoyer, and Marc’Aurelio Ranzato. Unsupervised machine translation using monolingual corpora only. *arXiv preprint arXiv:1711.00043*, 2017.
- [41] Piotr Bojanowski, Edouard Grave, Armand Joulin, and Tomas Mikolov. Enriching word vectors with subword information. *Transactions of the Association for Computational Linguistics*, 5: 135–146, 2017. ISSN 2307-387X.